Macromolecules

Volume 41, Number 6 March 25, 2008

Communications to the Editor

Morphological Study on an Azobenzene-Containing Liquid Crystalline Diblock Copolymer

Liming Ding, Huiming Mao, Ji Xu, Jinbo He, Xuan Ding, and Thomas P. Russell*

Department of Polymer Science & Engineering, University of Massachusetts, Amherst, Massachusetts 01003

Douglas R. Robello and Mark Mis

Research Laboratories, Eastman Kodak Company, Rochester, New York 14650

Received November 26, 2007

Revised Manuscript Received January 28, 2008

Diblock copolymers, BCPs, comprised of two chemically distinct blocks covalently bonded at one end, self-assemble into arrays of periodically ordered nanometer-sized microdomains.[1] Thin films made from coil−coil or rod−coil BCPs present a wide range of microphase-separated morphologies depending on the volume fraction of the components. By removing one block chemically by UV or ozone exposure, nanoporous templates are produced where the template pattern can be transferred to a substrate by reactive ion etching.[2] The fidelity of pattern transfer is very high since the film is in contact with the substrate. These nanotemplates are emerging as a simple, robust route for fabricating nanostructured materials.

Recently, amphiphilic liquid crystalline (LC) block copolymers have received attention because long-range order of the microdomains could be realized using optical or mechanical methods.[3,4] In particular, block copolymers containing azobenzene (Azo) units have been an active area of research.[5−7] Under irradiation, Azo polymers undergo an efficient photoisomerization: trans → cis *or* cis → trans. This photoresponsive property makes Azo block copolymers potentially useful for many applications, including photoswitches, photoalignment materials, photomechanical devices, photoinduced patterning,

* To whom correspondence should be addressed: Tel 413-545-2680; Fax 413-577-1510; e-mail Russell@mail.pse.umass.edu.

Scheme 1. Synthesis Routes for Azo Monomer (1), PEO Macroinitiator (2), and Diblock Copolymer (3)

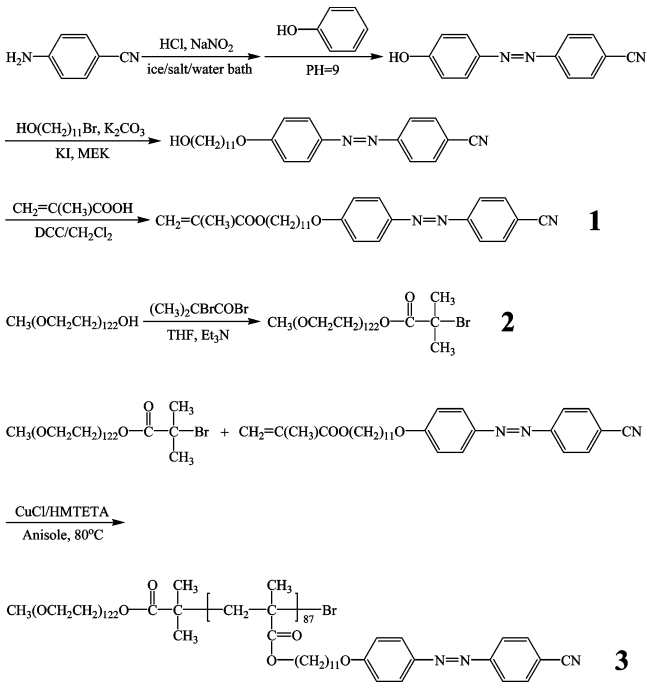

etc.[8,9] It was demonstrated by Ringsdorf et al. that electric field can orient Azo-containing LC copolymers.[10]

Iyoda et al. first synthesized an amphiphilic liquid crystalline diblock copolymer containing PEO as the hydrophilic block and a polymethacrylate with Azo side chains as the hydrophobic, liquid crystalline, and photoactive block.[3] Seki et al. developed a ABA-type triblock copolymer where A and B correspond to Azo-containing polymethacrylate and PEO, respectively.[4a] The morphology of a monolayer film of the triblock copolymer (trans form) on mica substrate showed nanoscopic dot and rod features. After UV irradiation, the film presented striped features. Thermal cis → trans isomerization at room temperature cause the stripes to revert to dots. Most recently, Ikeda et al. demonstrated, using a linearly polarized laser beam (488 nm), a parallel patterning

10.1021/ma702625c CCC: $40.75
Published on Web 02/19/2008

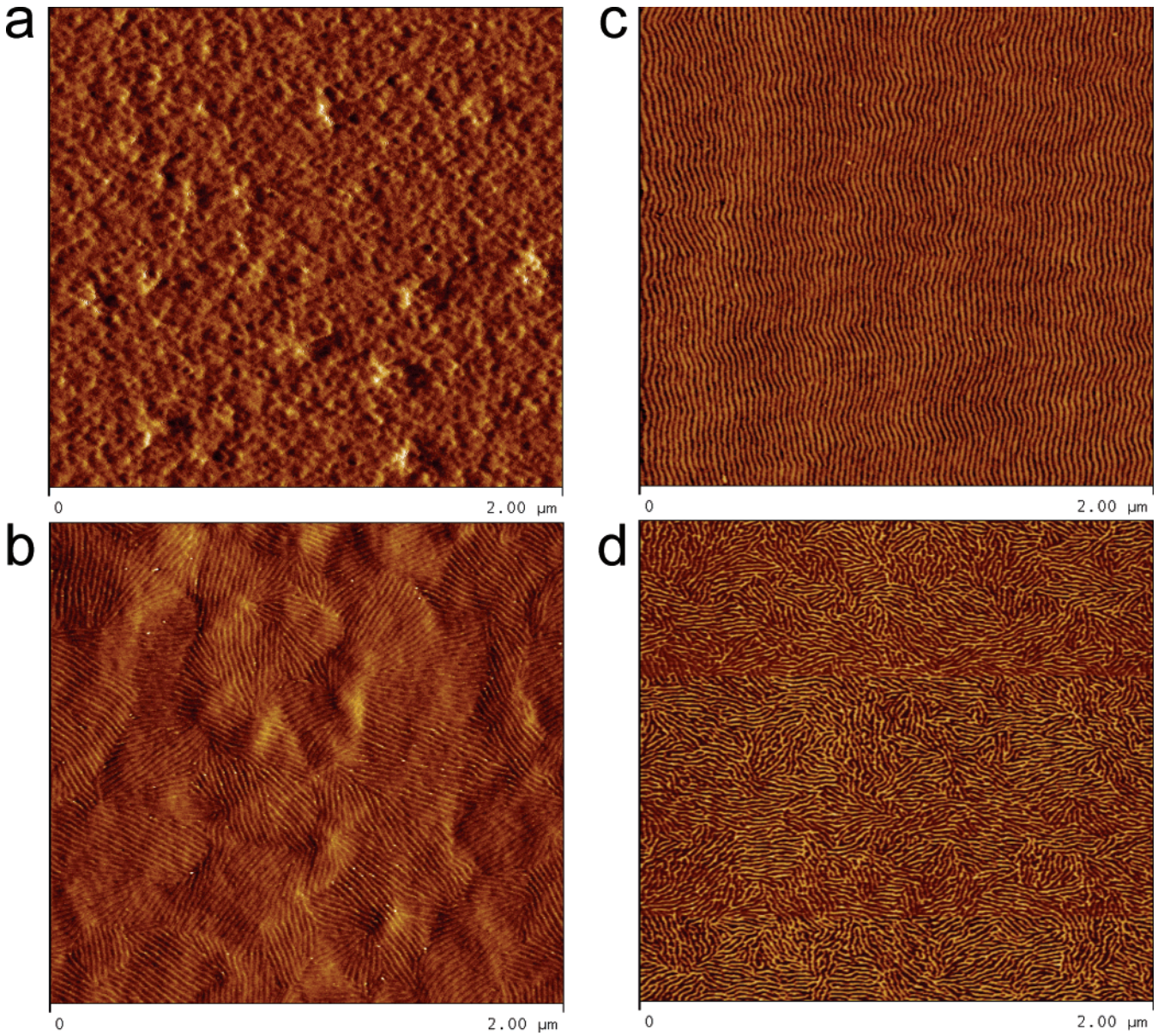

Figure 1. AFM phase images for 38.5 nm thick copolymer film on Si substrate. Thin films: (a) without any thermal annealing; (b) annealed at 140 °C for 1 day; (c) annealed at 180 °C for 1 day; (d) annealed at 180 °C for 2 days.

of PEO nanocylinders in the film of an amphiphilic diblock copolymer consisting of polymethacrylate block with Azo side chains.[4e] The PEO nanocylinders were aligned normal to the polarization direction of the light.

Here, we report, for an Azo diblock copolymer similar to that of Iyoda and Ikeda, the achievement of spontaneous alignment of nanocylinders by physical confinement within trenches on a substrate via annealing.

We synthesized an Azo-containing amphiphilic BCP by atom transfer radical polymerization (ATRP) following the work of Iyoda and Ikeda (see Scheme 1).[3,4e] Size exclusion chromatography (SEC) for the macroinitiator and the diblock copolymer are shown in Figure S1, and indicate successful growth of the Azo block with narrow polydispersity. Reverse phase HPLC analysis of the diblock copolymer showed it to be free of unreacted macroinitiator. ^{1}H NMR spectral analysis indicated that the PEO and Azo blocks have ~122 and ~87 repeat units, respectively (Figure S2), in good agreement with the SEC data. The molecular weight and polydispersity of the copolymer are 45.4K (M_n) and 1.17, respectively. Thermal gravimetric analysis (TGA) of the PEO macroinitiator showed only one decomposition event at 394.6 °C (Figure S3), while the diblock copolymer showed two (364.3 and 424.2 °C, Figure S4). The diblock copolymer exhibited only 1% weight loss up to 316 °C, demonstrating good thermal stability. Differential scanning calorimetry (DSC) of PEO macroinitiator indicated a melting point of 60.5 °C (Figure S5). For the diblock copolymer, the melting point of the PEO block decreased to 39.7 °C (Figure S6), consistent with the presence of the Azo block. The glass transition temperature (T_g) for the Azo block was measured to be ~33.2 °C. The other pair of peaks at 161.2 °C (on heating) and 155.9 °C (on cooling) in the DSC of the diblock copolymer are attributed to the smectic → isotropic and isotropic → smectic phase transitions of the liquid-crystalline Azo block, respectively.

Small-angle X-ray scattering (Figure S7) was used to characterize annealed drop-cast films (bulk). Three scattering peaks were observed with q ratio of the first three reflections of $1:\sqrt{3}:2$, suggesting a cylindrical microdomain morphology. A scattering peak at 1.4 nm^{-1} is seen, which can be attributed to the periodicity in the smectic phase (4.5 nm) of the Azo

group. The AFM image of the sheared film showed the appearance of the hexagonally packed PEO nanocylinders, further supporting the cylindrical microdomain morphology of the BCP (see Figure S8).

The phase behavior of bulk A−B diblock copolymers is determined by three factors: the degree of polymerization, the overall volume fraction of the components, and the Flory−Huggins segmental interaction parameter, χ.[11] However, many other factors influence the morphology of thin films, for example substrate, film thickness, annealing conditions, and interfacial interactions.[12]

In Ikeda's work,[4e] annealing a 100 nm thick film on a glass substrate at 140 °C produced PEO nanocylinders oriented normal to the surface. Here, the alignment behavior of the LC diblock copolymer in trenches was of interest, but we first studied the film structure on an unpatterned substrate. Thin films, ∼38.5 nm in thickness, of the Azo BCP were prepared by spin-coating from a toluene/THF solution (volume ratio 1:1) onto Si substrates coated with 2500 Å wet thermal oxide. The morphologies of the films annealed under different conditions were studied by scanning force microscopy, as shown in Figure 1.

The dried copolymer film without any thermal annealing presented a disordered microstructure without a well-defined microphase-separated morphology, since the self-assembly of the BCP could not reach an equilibrium morphology during the rapid spin-coating process (see Figure 1a). Parts b and c of Figure 1 show the morphologies of the copolymer films annealed in vacuo at 140 and 180 °C for 1 day, respectively. It should be noted that all AFM images presented here are phase images obtained by using tapping mode. The dark parts in the images are PEO domains. Increasing the annealing temperature, the alignment of the cylindrical microdomains improved, and the lateral ordering increased. Factors influencing the evolution of the morphology include the microphase separation between the PEO block and the Azo block, the isotropic → smectic phase transition of Azo block, and PEO crystallization. Being annealed at temperatures above the glass transition temperature of the Azo block, the self-assembly and microphase separation led to a strong alignment of the microdomains. When annealed at 180 °C, since the temperature exceeds the smectic → isotropic phase transition temperature (161.2 °C), both blocks of the copolymer are liquidlike. The PEO block and the Azo block have sufficient mobility to self-assemble. By gradually decreasing the temperature, the Azo block first undergoes the isotropic → smectic phase transition, and then microphase separation with the PEO block occurs. The rigid-rod-like Azo units easily pack uniformly and can propagate this order over large distances (Figure 1c). When temperature goes below the PEO melting point (39.7 °C), the PEO block crystallizes between the hard Azo microdomain. The self-assembly and microphase separation lead to a long-range ordering of the PEO nanocylinders (Figure S9). 2D FFT analysis of Figure S9 indicates that the periodicity of the microdomain is ∼23.3 nm (Figure S10), and the calculated *d*-spacing (20.2 nm) is fully consistent with the SAXS results (20.0 nm) (see Figure S7). Figure 1d shows the morphology of the copolymer film that was annealed at 180 °C for 2 days. There is no long-range order, which may result from a thermal cross-linking and degradation.

Nealey, Sibener, Ross, and Kramer et al.[2c,13−16] have spin-coated lamellae-, cylinder-, and sphere-forming BCPs on topographically patterned substrates and investigated the effects of confinement on the thin film morphology. They used grooves (gratings or channels) to direct the alignment of the nanodomains

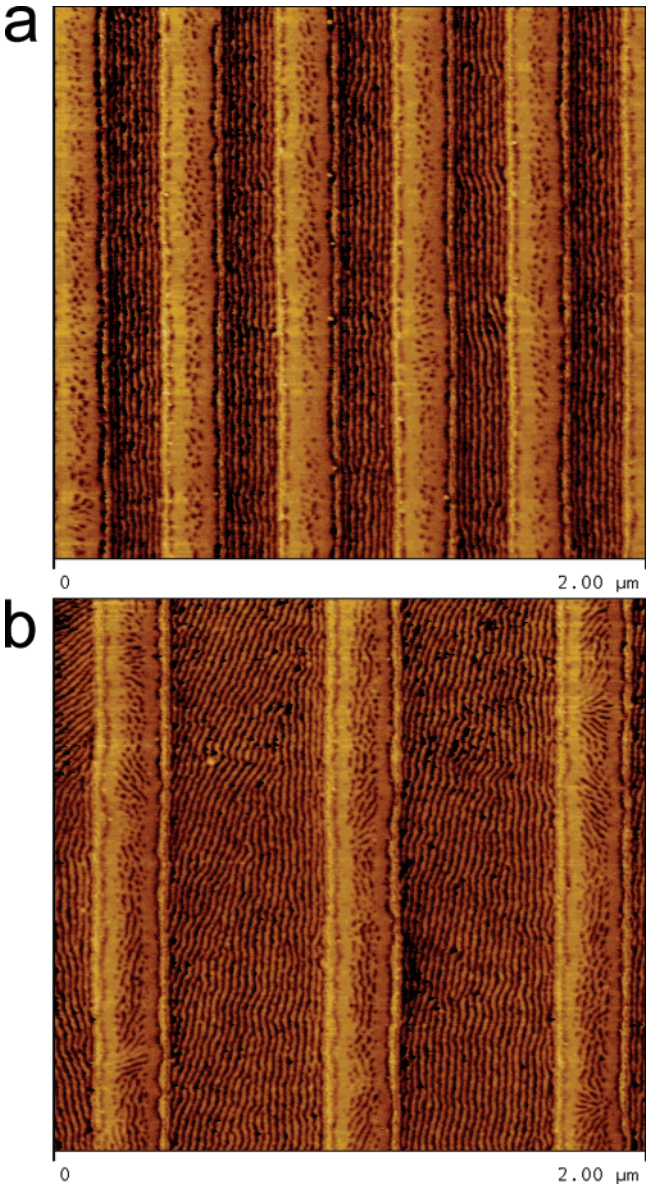

Figure 2. AFM images of the annealed diblock copolymer films inside the trenches: (a) 207 nm wide trench; (b) 582 nm wide trench.

and promote lateral ordering in BCP thin films. In this work, to improve the lateral ordering of the cylindrical nanodomains oriented parallel to the substrate, the BCP films were placed on surfaces having trenches with different sizes. The trench bottom width varied from 105 to 461 nm while the top width varied from 207 to 582 nm, and the depth was 55−60 nm (Figures S11 and S12). It is obvious that, instead of the wavy orientation shown in Figure 1c, the nanodomains aligned due to the confinement in the trenches, as shown in Figure 2a,b. Significantly improved alignment was seen in the narrower trenches. During the annealing, the polymer might flow into the trenches, leaving a very thin layer on the surface of the substrate between the trenches.

In summary, liquid crystalline cylinder-forming BCPs were synthesized. In thin films the cylindrical microdomains oriented parallel to the substrate. The alignment of the PEO microdomains was significantly improved by increasing the annealing temperature. When deposited on patterned surfaces followed by annealing, alignment of the nanocylinders along the grooves occurred, induced by physical confinement. Different technical approaches aiming to improve the alignment of nanocylinders

and to realize long-range order in diblock copolymer films are underway.

Acknowledgment. This work is supported by the Department of Energy, Division of Materials Research, under DE-FG-02-ER45998. We thank Dr. Shiying Zheng of Eastman Kodak Company and Dr. Jian Wu of University of Massachusetts for technical assistance and valuable discussions. The Si wafers inscribed with trenches were kindly provided by Seagate Technology. Technical assistance provided by Kim Le, Dr. Thomas H. Mourey, James Hauenstein, and Dr. J. Michael Hewitt of Eastman Kodak Company on SEC, HPLC, and NMR is acknowledged.

Supporting Information Available: Experimental details. This material is available free of charge via the Internet at http://pubs.acs.org.

References and Notes

(1) (a) Chen, J. T.; Thomas, E. L.; Ober, C. K.; Mao, G. P. *Science* **1996**, *273*, 343. (b) Morkved, T. L.; Lu, M.; Urbas, A. M.; Ehrichs, E. E.; Jaeger, H. M.; Mansky, P.; Russell, T. P. *Science* **1996**, *273*, 931. (c) Bates, F. S.; Fredrickson, G. H. *Phys. Today* **1999**, *52*, 32.

(2) (a) Hawker, C. J.; Russell, T. P. *MRS Bull.* **2005**, *30*, 952. (b) Park, M.; Harrison, C.; Chaikin, P. M.; Register, R. A.; Adamson, D. H. *Science* **1997**, *276*, 1401. (c) Cheng, J. Y.; Ross, C. A.; Thomas, E. L.; Smith, H. I.; Vancso, G. J. *Appl. Phys. Lett.* **2002**, *81*, 3657.

(3) Tian, Y.; Watanabe, K.; Kong, X.; Abe, J.; Iyoda, T. *Macromolecules* **2002**, *35*, 3739.

(4) (a) Kadota, S.; Aoki, K.; Nagano, S.; Seki, T. *J. Am. Chem. Soc.* **2005**, *127*, 8266. (b) Yu, H.; Shishido, A.; Ikeda, T.; Iyoda, T. *Macromol. Rapid Commun.* **2005**, *26*, 1594. (c) Morikawa, Y.; Nagano, S.; Watanabe, K.; Kamata, K.; Iyoda, T.; Seki, T. *Adv. Mater.* **2006**, *18*, 883. (d) Yu, H.; Li, J.; Ikeda, T.; Iyoda, T. *Adv. Mater.* **2006**, *18*, 2213. (e) Yu, H.; Iyoda, T.; Ikeda, T. *J. Am. Chem. Soc.* **2006**, *128*, 11010.

(5) (a) Mao, G.; Wang, J.; Clingman, S. R.; Ober, C. K.; Chen, J. T.; Thomas, E. L. *Macromolecules* **1997**, *30*, 2556. (b) Osuji, C. O.; Chen, J. T.; Mao, G.; Ober, C. K.; Thomas, E. L. *Polymer* **2000**, *41*, 8897. (c) You, F.; Paik, M. Y.; Häckel, M.; Kador, L.; Kropp, D.; Schmidt, H. W.; Ober, C. K. *Adv. Funct. Mater.* **2006**, *16*, 1577. (d) Paik, M. Y.; Krishnan, S.; You, F.; Li, X.; Hexemer, A.; Ando, Y.; Kang, S. H.; Fischer, D. A.; Kramer, E. J.; Ober, C. K. *Langmuir* **2007**, *23*, 5110.

(6) (a) Breiner, T.; Kreger, K.; Hagen, R.; Häckel, M.; Kador, L.; Müller, A. H. E.; Kramer, E. J.; Schmidt, H. W. *Macromolecules* **2007**, *40*, 2100. (b) Häckel, M.; Kador, L.; Kropp, D.; Schmidt, H. W. *Adv. Mater.* **2007**, *19*, 227.

(7) Hayakawa, T.; Horiuchi, S.; Shimizu, H.; Kawazoe, T.; Ohtsu, M. *J. Polym. Sci., Part A: Polym. Chem.* **2002**, *40*, 2406.

(8) (a) Yager, K. G.; Barrett, C. J. *J. Chem. Phys.* **2007**, *126*, 094908/1. (b) Yager, K. G.; Barrett, C. J. *Polym. Nanostruct. Their Appl.* **2007**, *2*, 243. (c) Yager, K. G.; Barrett, C. J. *Macromolecules* **2006**, *39*, 9320. (d) Yager, K. G.; Barrett, C. J. *J. Photochem. Photobiol., A: Chem.* **2006**, *182*, 250. (e) Tanchak, O. M.; Barrett, C. J. *Macromolecules* **2005**, *38*, 10566.

(9) (a) Zhao, Y. *Polym. Nanostruct. Their Appl.* **2007**, *2*, 281. (b) Cui, L.; Zhao, Y.; Yavrian, A.; Galstian, T. *Macromolecules* **2003**, *36*, 8246. (c) Wang, G.; Tong, X.; Zhao, Y. *Macromolecules* **2004**, *37*, 8911. (d) Tong, X.; Wang, G.; Yavrian, A.; Galstian, T.; Zhao, Y. *Adv. Mater.* **2005**, *17*, 370. (e) Sevigny, S.; Bouchard, L.; Motallebi, S.; Zhao, Y. *Liq. Cryst.* **2005**, *32*, 599. (f) Tong, X.; Wang, G.; Soldera, A.; Zhao, Y. *J. Phys. Chem. B* **2005**, *109*, 20281.

(10) (a) Ringsdorf, H.; Zentel, R. *Makromol. Chem.* **1982**, *183*, 1245. (b) Ringsdorf, H.; Schmidt, H. W. *Makromol. Chem.* **1984**, *185*, 1327.

(11) Bates, F. S.; Fredrickson, G. H. *Annu. Rev. Phys. Chem.* **1990**, *41*, 525.

(12) (a) Fasolka, M. J.; Mayes, A. M. *Annu. Rev. Mater. Res.* **2001**, *31*, 323. (b) Segalman, R. A. *Mater. Sci. Eng., R* **2005**, *R48*, 191.

(13) (a) Stoykovich, M. P.; Nealey, P. F. *Mater. Today* **2006**, *9*, 20. (b) Park, S.; Stoykovich, M. P.; Ruiz, R.; Zhang, Y.; Black, C. T.; Nealey, P. F. *Adv. Mater.* **2007**, *19*, 607.

(14) (a) Sundrani, D.; Sibener, S. J. *Macromolecules* **2002**, *35*, 8531. (b) Sundrani, D.; Darling, S. B.; Sibener, S. J. *Nano Lett.* **2004**, *4*, 273. (c) Sundrani, D.; Darling, S. B.; Sibener, S. J. *Langmuir* **2004**, *20*, 5091.

(15) (a) Chuang, V. P.; Cheng, J. Y.; Savas, T. A.; Ross, C. A. *Nano Lett.* **2006**, *6*, 2332. (b) Cheng, J. Y.; Zhang, F.; Smith, H. I.; Vancso, G. J.; Ross, C. A. *Adv. Mater.* **2006**, *18*, 597. (c) Cheng, J. Y.; Ross, C. A.; Smith, H. I.; Thomas, E. L. *Adv. Mater.* **2006**, *18*, 2505.

(16) (a) Segalman, R. A.; Yokoyama, H.; Kramer, E. J. *Adv. Mater.* **2001**, *13*, 1152. (b) Hammond, M. R.; Kramer, E. J. *Macromolecules* **2006**, *39*, 1538. (c) Stein, G. E.; Lee, W. B.; Fredrickson, G. H.; Kramer, E. J.; Li, X.; Wang, J. *Macromolecules* **2007**, *40*, 5791.

MA702625C